J|A|C|S COMMUNICATIONS

Published on Web 04/01/2009

Magnetic Transition and Long-Time Relaxation Behavior Induced by Selective Injection of Guest Molecules into Clathrate Hydrates

Youngjune Park,[†] Joonghoe Dho,[‡] Jiwoong Seol,[†] Sun-Hwa Yeon,[†] Minjun Cha,[†] Y. H. Jeong,[§] Yongwon Seo,[||] and Huen Lee*,[†]

Department of Chemical and Biomolecular Engineering, Korea Advanced Institute of Science and Technology (BK-Program), 373-1 Guseong-dong, Yuseong-gu, Daejeon 305-701, Republic of Korea, Department of Physics, Kyungpook National University, Daegu 702-701, Republic of Korea, Department of Physics and Electron Spin Science Center, Pohang University of Science and Technology, Pohang 790-784, Republic of Korea, and Department of Chemical Engineering, Changwon National University, 9 Sarim-dong, Changwon, Gyeongnam 641-773, Republic of Korea

Received February 5, 2009; E-mail: h_lee@kaist.ac.kr

Versatile nanostructures, including metal−organic frameworks and carbon-based materials, have been designed and synthesized for specific targets of material science and engineering. More significantly, several recent studies have reported the adsorption of magnetic molecules on a nanostructured surface and highlighted the unusual magnetic properties of these arrangements. The unique inclusion and coupling phenomena of gaseous magnetic guest molecules into low-dimensional microphases of nanostructured surfaces have been detected in the configurations of cages, tubes, and wires with the aim of controlling the properties of the material, including its magnetism or reactivity, thereby creating unusual and discrete magnetic patterns. In addition, magnetic O_2 molecules reveal distinctive magnetic behavior when they undergo 3D solidification of the α, β, and γ phases or when they occupy the empty enclosing spaces of clathrate crystals such as a β-quinol compound.[1−5] In the past few years, multiple studies of O_2 magnetism have confirmed that low-dimensional O_2 confinement in nanostructures such as the 2D O_2-filled nanostructure in graphite and 1D O_2 dimers adsorbed in metal−organic frameworks substantially but not completely destroy the inherent antiferromagnetism of pure solid O_2.[6−10]

Here we demonstrate that the selective injection of magnetic O_2 and nonmagnetic tetrahydrofuran (THF) molecules into the water-ice cages of clathrate hydrates can modify the inherent magnetism. Ripmeester et al.[11] examined the spin−lattice relaxation of THF clathrate hydrate in the presence of O_2, analyzing its NMR behavior. However, the present study is focused on revealing two unique phenomena of the magnetic transition (antiferromagnetic to ferromagnetic) and long-time relaxation occurring in these clathrate hydrates. First, the binary THF and O_2 clathrate hydrate [(THF + O_2)*] was synthesized by exposing O_2 molecules to pure THF clathrate hydrate [(THF)*], with the occupation of magnetic O_2 in sII-S (5^{12}, cage occupancy $\theta_{S,O_2} \approx 0.4$) and nonmagnetic THF in sII-L ($5^{12}6^4$, $\theta_{L,THF} \approx 1.0$). On the other hand, the pure O_2 clathrate hydrate [(O_2)*] forms stably by enclosing magnetic O_2 in both sII-S ($\theta_{S,O_2} \approx 0.8$) and sII-L ($\theta_{L,O_2} \approx 1$). The crystalline structure and guest occupancy of these clathrate hydrates were analyzed using neutron powder diffraction [Figure S1 in the Supporting Information (SI)]. The icy magnetic 3D superstructure is composed of two magnetic sublattices, namely, a tetrahedral sublattice formed by the sII-S cages and a diamond-like sublattice formed by the sII-L cages (Figure 1), as clearly observed in antiferromagnetic materials and the pyrochlore lattices of spin-ice materials.[12] More specifically, the confined magnetic O_2 molecules that constitute a 3D channel induce two different clathrate hydrates to create a tetrahedral sublattice [(THF + O_2)*] and both tetrahedral and diamond-like sublattices [(O_2)*]. Here, (THF + O_2)* reveals a relatively low O_2 population in an icy crystalline matrix, resulting in the creation of a substantial number of empty cage sites neighboring the confined O_2 molecules with imperfect 3D channels.

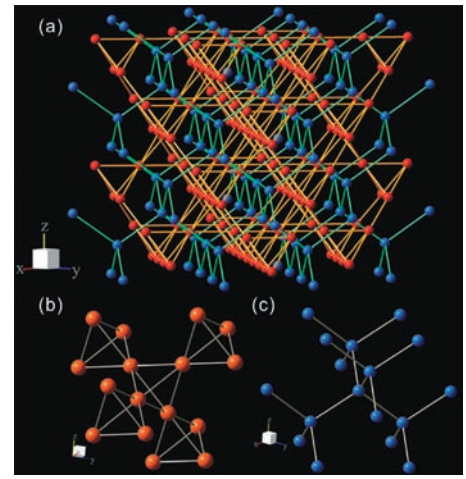

Figure 1. (a) Superstructure composed of guest molecules in both sII-S (orange balls) and sII-L cages (blue balls). (b) Tetrahedral sublattice composed of O_2 molecules in sII-S cages. Remarkably, the O_2 molecules filled in the sII-S cages form a network of 1D molecular oxygen chains along the centers of the sII-S cages, thus creating a pyrochlore superstructure of corner-sharing tetrahedral elements that closely follows the spin-ice materials of $Ho_2Ti_2O_7$ and $Dy_2Ti_2O_7$. (c) Diamond-like sublattice composed of THF or O_2 molecules in sII-L cages. In (a)−(c), the line connections between two molecules do not represent chemical bonds but instead are eye-guides to show the 3D superstructure clearly.

In order to explore the magnetic properties of O_2 in clathrate hydrates, magnetic susceptibility [$\chi(T)$] was measured. Powder samples were packed into a quartz tube and then mounted on a Quantum Design Magnetic Property Measurement System (MPMS) or Physical Property Measurement System (PPMS) at 150 K. The measured ac/dc magnetic properties of O_2 molecules forming the sII 3D superstructures of (THF + O_2)* and (O_2)* are identified as completely different from the antiferromagnetism of solid or confined 1D or 2D O_2 reported previously (Figure S2 in the SI). For (THF + O_2)* and (O_2)*, the dc magnetic susceptibility [$\chi_{dc}(T)$]

[†] Korea Advanced Institute of Science and Technology.
[‡] Kyungpook National University.
[§] Pohang University of Science and Technology.
[||] Changwon National University.

10.1021/ja9009088 CCC: $40.75

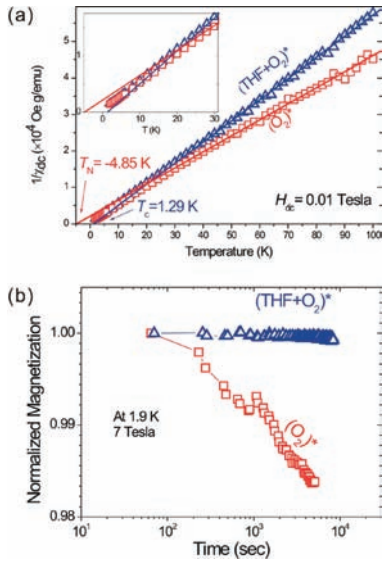

Figure 2. (a) Plots of $1/\chi_{dc}(T)$ vs T for (THF + O_2)* and (O_2)* measured at H_{dc} = 0.01 T; the inset shows a magnified view of low-temperature region. The solid lines are the Curie−Weiss fits to the measured data over the temperature range 20−100 K. (b) Long-time relaxation behavior of the magnetization $M(t)$ for (THF + O_2)* and (O_2)*. The sample was initially cooled to 1.9 K under 0 T, and then the magnetization was measured as a function of time after setting the field to 7 T.

curves appear to be nearly paramagnetic, but they display a slightly different feature compared with typical paramagnets in the low-temperature region. The zero-field O_2 magnetic moments tend to be aligned randomly as a result of thermal fluctuations, while the high-field (7 T) ones imply field-induced alignment. A clear dissimilarity might be extracted by considering the simple Curie−Weiss law.

The $1/\chi(T)$ curve for (THF + O_2)* shows an upward deviation from linearity in the low-temperature region, while a slight downward tendency is observed for (O_2)* (Figure 2a and Figure S3 in the SI). From the fits to the Curie−Weiss law [$1/\chi \propto (T - T_{C,N})$, where $T_{C,N}$ represents either the Curie temperature T_C or the Neél temperature T_N], the $1/\chi(T)$ for (THF + O_2)* was observed to exhibit ferromagnetic-like behavior with T_C = +3.25 K (ac) and +1.29 K (dc). In contrast, the antiferromagnetic-like feature appears for (O_2)*, with T_N = −4.45 K (ac) and −4.85 K (dc). For a clearer understanding of the contradictory magnetic patterns of (THF + O_2)* and (O_2)*, which have identical structures (cubic, $Fd3m$) but exhibit dissimilar O_2 populations, the magnetic interactions in each clathrate hydrate must be taken into account. The O_2 molecules in (THF + O_2)* are characterized by negligible magnetic coupling between neighboring molecules, as in a typical paramagnet, leading to field-induced saturation behavior as in typical ferromagnets. In contrast, a weak antiferromagnetic interaction between O_2 molecules prevails in (O_2)*. This unique magnetic pattern comes from either direct coupling between guest O_2 molecules behaving dynamically in linear nanochannels consisting of consecutively stacked cages, indirect coupling between host and guest oxygens, or both.

Furthermore, a distinctive magnetic property difference between (THF + O_2)* and (O_2)* can be seen directly from the field-dependent magnetization [$M(H)$] patterns. (THF + O_2)* possesses 6.4 O_2 molecules/unit cell on average ($6.4O_2 \cdot 8THF \cdot 136H_2O$), whereas ($O_2$)* has 20.8 O_2 molecules/unit cell ($20.8O_2 \cdot 136H_2O$ with a 15 wt % hexagonal ice phase: 12.8 O_2 in sII-S and 8 O_2 in sII-L). At this stage, a key question arises, namely, how the magnetization values [1.95 μ_B/O_2 for (THF + O_2)* and 0.81 μ_B/O_2 for (O_2)*] significantly differ at 1.9 K and 7 T, where saturated magnetization is observed (Figure S4 in the SI). Surprisingly, it was found that the occupancy number of O_2 in (O_2)* is much higher than that in (THF + O_2)*, despite the fact that their magnetization values are reversed. These magnetic data indicate that the O_2 populations in the small and large cages greatly affect the magnetic coupling of (THF + O_2)* and (O_2)*, and thus, their distinct magnetic patterns were observed. In particular, the magnetization was measured as a function of time at 7 T and 1.9 K (Figure 2b). This long-time relaxation of magnetization [$M(t)$] also supports the dissimilarity between the magnetic property patterns of (THF + O_2)* and (O_2)*. A significant feature is that the (O_2)* magnetization decreases as time elapses, whereas the (THF + O_2)* value remains constant. In contrast to the zero- or positive-slope $M(t)$ of typical ferromagnets or spin-glasses, such a negative time dependence of the (O_2)* magnetization strongly suggests a rearrangement of oxygen magnetic moments to minimize the total magnetic energy in an antiferromagnetic-like system.[13,14] Interestingly, this molecular inclusion phenomenon may be exploited via the lattice or in molecular engineering to tune the host−guest interaction pattern of a clathrate hydrate matrix to synthesize ice-based magnetic materials. In terms of both science and engineering, water-ice-based clathrate hydrate structures are expected to open up new opportunities to develop functionalized icy materials with specific targets, as demonstrated here for the confined O_2 molecules forming the 3D superstructures of crossed X-channels.

Acknowledgment. This work was supported by the Korea Science and Engineering Foundation (KOSEF) through the National Research Laboratory Program [R0A-2005-000-10074-0(2008)], the Nuclear R&D Program (M20802000297-08B0200-29710), the WCU Program (31-2008-000-10055-0) funded by the Ministry of Education and Science & Technology (MEST), and the HRHR Project funded by KAIST.

Supporting Information Available: Sample preparation details, experimental procedures, neutron powder diffraction patterns, and $\chi(T)$ and $M(H)$ plots. This material is available free of charge via the Internet at http://pubs.acs.org.

References

(1) Freiman, Y. A.; Jodl, H. J. *Phys. Rep.* **2004**, *401*, 1–228.
(2) Evans, D. F.; Richards, R. E. *Nature* **1952**, *170*, 246.
(3) Cooke, A. H.; Meyer, H.; Wolf, W. P. *Proc. R. Soc. London, Ser. A* **1954**, *225*, 112–122.
(4) Meyer, H.; O'Brien, M. C. M.; Van Vleck, J. H. *Proc. R. Soc. London, Ser. A* **1957**, *243*, 414.
(5) Foner, S.; Meyer, H.; Kleiner, W. H. *J. Phys. Chem. Solids* **1961**, *18*, 273–285.
(6) Kitaura, R.; Kitagawa, S.; Kubota, Y.; Kobayashi, T. C.; Kindo, K.; Mita, Y.; Matsuo, A.; Kobayashi, M.; Chang, H.-C.; Ozawa, T. C.; Suzuki, M.; Sakata, M.; Takata, M. *Science* **2002**, *298*, 2358–2361.
(7) Mori, W.; Kobayashi, T. C.; Kurobe, J.; Amaya, K.; Narumi, Y.; Kumada, T.; Kindo, K.; Katori, H. A.; Goto, T.; Miura, N.; Takamizawa, S.; Nakayama, H.; Yamaguchi, K. *Mol. Cryst. Liq. Cryst.* **1997**, *306*, 1–7.
(8) Kobayashi, T. C.; Matsuo, A.; Suzuki, M.; Kindo, K.; Kitaura, R.; Matsuda, R.; Kitagawa, S. *Prog. Theor. Phys. Suppl.* **2005**, *159*, 271–279.
(9) Takamizawa, S.; Nakata, E.; Akatsuka, T. *Angew. Chem., Int. Ed.* **2006**, *45*, 2216–2221.
(10) Köbler, U.; Marx, R. *Phys. Rev. B* **1987**, *35*, 9809–9816.
(11) Ripmeester, J. A.; Garg, S. K.; Davidson, D. W. *J. Magn. Reson.* **1980**, *38*, 537–544.
(12) (a) Pauling, L. *J. Am. Chem. Soc.* **1935**, *57*, 2680–2684. (b) Snyder, J.; Slusky, J. S.; Cava, R. J.; Schiffer, P. *Nature* **2001**, *413*, 48–51.
(13) Dho, J.; Kim, W. S.; Hur, N. H. *Phys. Rev. Lett.* **2002**, *89*, 027202.
(14) Muraoka, Y.; Tabata, H.; Kawai, T. *Appl. Phys. Lett.* **2000**, *76*, 1179–1181.

JA9009088